

OPTICAL FIELDS

PACS numbers: 42.25.Hz; 42.30.–d; 42.87.–d
DOI: 10.1070/QE2013v043n10ABEH015187

Longitudinal correlation properties of an optical field with broad angular and frequency spectra and their manifestation in interference microscopy

D.V. Lyakin, V.P. Ryabukho

Abstract. **The results of theoretical and experimental studies of the longitudinal correlation properties of an optical field with broad angular and frequency spectra and manifestations of these properties in interference microscopy are presented. The joint and competitive influence of the angular and frequency spectra of the object-probing field on the longitudinal resolution and on the amplitude of the interference microscope signals from the interfaces between the media inside a multilayer object is demonstrated. The method of compensating the so-called defocusing effect that arises in the interference microscopy using objectives with a large numerical aperture is experimentally demonstrated, which consists in using as a light source in the interference microscope an illuminating interferometer with a frequency-broadband light source. This method of compensation may be used as the basis of simultaneous determination of geometric thickness and refractive index of media forming a multilayer object.**

Keywords: *interference microscopy, frequency-broadband light sources, longitudinal correlation properties of optical field.*

1. Introduction

In the low-coherence interferometry, optical coherence tomography and interference microscopy that use broadband extended light sources, the effects of interference of partially coherent light with essentially limited spatial correlation lengths are observed. In these methods the parameters of the measured signals, i.e., the interference signals and images, are determined by the correlation properties of the interfering fields. In most methods the informative signals are determined by the longitudinal correlation properties of the optical fields that are determined either by the frequency properties of the fields or by a combination of frequency and angular spectra or by the parameters of the angular spectrum solely, the frequency spectrum being narrow enough.

The longitudinal correlation of a wave field describes the coherence of its oscillations at two points $P_1(z)$ and $P_2(z + \Delta z)$ along the principal direction of the field propagation (the z axis in Fig.1.). If there is a time delay Δt between the oscillations at the points P_1 and P_2, then it is common to consider longitudinal spatiotemporal correlation of the field oscillations. If $\Delta t = 0$, the longitudinal spatial correlation of the field is considered.

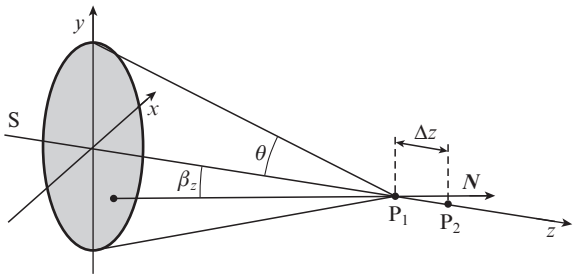

Figure 1. To the definition of field correlation in the longitudinal direction: S is the extended light source; P_1 and P_2 are the points at the z axis; β_z is the angle between the direction of propagation $\boldsymbol{N}$ of a certain spatial component of the field and the z axis; $\theta = \max(\beta_z)$ is the angular aperture of the field (angular dimensions of the source) at the point of observation.

Within the frameworks of classical conceptions [1, 2] the longitudinal spatial correlation is identified with the temporal correlation (temporal coherence) of the wave field oscillations, the relative time delay of these oscillations being expressed as $\Delta t = \Delta z/c$, where c is the velocity of the field propagation. Therefore, within the frameworks of these conceptions the longitudinal spatial correlation is determined by the frequency spectrum of the wave field source. Correspondingly, the length L_c of the longitudinal correlation of the wave field within the frameworks of classical conceptions is assumed to be identically equal to the length l_c of the temporal coherence, determined by the width $\Delta\omega$ of the frequency spectrum:

$$L_c \equiv l_c \sim 2\pi/\Delta\omega. \quad (1)$$

This classical conception of longitudinal correlation of a wave field appears to be incorrect for the field, the individual components of which (plane waves) propagate at different angles β_z with respect to the principal direction z of field propagation, i.e., when the wave field possesses an angular spectrum of finite width [3–10] determined by the angular aperture of the field θ (Fig. 1). Such wave fields arise, e.g., when the source is an extended luminous body, or when the field is formed by an optical imaging system with a large numerical aperture. The fields with extremely large angular apertures (extremely broad angular spectrum) are produced in the high-resolution interference microscopy [11–14] using wide-aperture objectives.

D.V. Lyakin, V.P. Ryabukho Institute of Precision Mechanics and Control, Russian Academy of Sciences, ul. Rabochaya 24, 410028 Saratov, Russia; N.G. Chernyshevsky Saratov State University, ul Astrakhanskaya 83, 410012 Saratov, Russia;
e-mail: LDV-77@mail.ru, rvp-optics@yandex.ru

Received 28 March 2013
Kvantovaya Elektronika **43** (10) 949–957 (2013)
Translated by V.L. Derbov

In Refs [3, 4, 6, 7], using the generalisation of the Van Cittert–Zernike theorem over the case of longitudinal arrangement of the points, between which the correlation of the wave field generated by an extended quasi-monochromatic ($\Delta\omega \to 0$) source is considered, the notion of longitudinal spatial correlation (coherence) is introduced that is determined only by the angular spectrum of the field in the observation area. Within the frameworks of the paraxial approximation the expression is derived [3, 4] for the length of longitudinal spatial correlation of a quasi-monochromatic wave field, determined by the angular aperture of the field θ:

$$L_c = \rho_{\|} \sim 2\lambda_0/\theta^2, \tag{2}$$

where λ_0 is the wavelength of the quasi-monochromatic radiation. A similar expression is found in [5] from the generalisation of the Wiener–Khintchin theorem over the spatiotemporal correlations of random wave fields. One should note, that the result analogous in fact, but formulated in terms of the field spectral coherence degree in a pair of axial points, was obtained in Ref. [8] considering a radiometric model of coherence propagation in space.

A clear visualisation of the regions of longitudinal coherence of a quasi-monochromatic wave field and their transformation when moving off the source is provided by the pattern of longitudinal speckles, formed in the scattered laser field [9].

During the last few years the phenomenon of longitudinal spatial correlation determined by the broad angular spectrum of the field is extensively studied both theoretically and experimentally. Experimentally it was demonstrated that the length of longitudinal correlation of the field from a thermal source can be determined by its angular spectrum [10]. The methods of surface profilometry, based on the use of longitudinal spatial correlation of the fields from quasi-monochromatic (laser) sources have been developed [15–17]. The problem of the correlation length limitation in the longitudinal direction of the field generated by a thermal source, caused by its broad angular spectrum, arises and is being studied in the case of forming coincident images (ghost imaging) [18, 19]. In the theory of interference microscopy several approaches are being developed, in which the influence of the broad angular spectrum of the light on the interference signal is taken into account in the case of depth-resolved probing of layered objects [20–26]. However, these approaches are based on the concept of separate influence of the temporal coherence (more correctly, the frequency spectrum) and the longitudinal spatial correlation, determined by the angular spectrum, on the interference microscope signal.

Thus, two conceptions of the longitudinal correlation of a wave field have been elaborated. In the case of a source with a broad frequency spectrum it is identified with the temporal coherence and, therefore, is determined by the width of the frequency spectrum $\Delta\omega$. In the case of a quasi-monochromatic source ($\Delta\omega \to 0$) it is identified with the longitudinal spatial coherence, determined by the angular aperture of the field θ. The gap between these two conceptions, that becomes evident when considering a wave field with both the frequency and the angular spectra being broad, makes it necessary to formulate a physical conception, considering the longitudinal correlation of the wave field as a longitudinal spatial correlation, determined by the combined and competitive influence of the frequency and angular spectra of the field.

This paper presents the results of our theoretical and experimental studies of the longitudinal spatial correlation of the optical field, caused by the combined and competitive influence of the finite width of both the frequency and angular spectra, and its manifestation in the interferometry of longitudinal shift with the amplitude division of the initial field from an extended frequency-broadband source. We also extend our physical conceptions of longitudinal correlation properties of the fields with broad frequency and angular spectra over the fields that are obtained in the high-resolution interference microscopy and experimentally demonstrate a number of effects of combined and competitive influence of the frequency and angular spectra on the interference microscope signal.

2. The function and the length of longitudinal spatial correlation of a field with broad frequency and angular spectra

In Ref. [5] expression (9.27) is derived for the spatiotemporal correlation function of the uniform and stationary random field at two arbitrary spatial points $P_1(\boldsymbol{r}_1)$ and $P_2(\boldsymbol{r}_2)$:

$$\Psi(\Delta t, \Delta \boldsymbol{r}) = \int_0^\infty \oint J(\omega, \boldsymbol{N}) \exp[\mathrm{i}(k\boldsymbol{N}\Delta\boldsymbol{r} - \omega\Delta t)]\, \mathrm{d}\Omega(\boldsymbol{N})\, \mathrm{d}\omega, \tag{3}$$

where $k = \omega/c$ is the wavenumber; $\boldsymbol{N}$ is the unit vector defining the direction of propagation of a certain angular component of the field; $\Delta t = t_1 - t_2$ is the time delay of the oscillations at the points P_1 and P_2; $\Delta\boldsymbol{r} = \boldsymbol{r}_1 - \boldsymbol{r}_2$; $J(\omega, \boldsymbol{N})$ is the ray intensity, i.e., the quantity that describes the frequency-angular spectrum of the field; and $\mathrm{d}\Omega(\boldsymbol{N})$ is the solid angle element.

From Eqn (3) it is possible to derive the expression for the longitudinal spatiotemporal correlation function of the field generated by a source having the form of a planar disc by performing the substitution $\boldsymbol{N}\Delta\boldsymbol{r} = \cos(\beta_z)\Delta z$, $\mathrm{d}\Omega(\boldsymbol{N}) = \sin(\beta_z)\mathrm{d}\beta_z\mathrm{d}\varphi$:

$$\Psi_{\|}(\Delta t, \Delta z) = 2\pi \int_0^\infty \int_0^\theta J(\omega, \beta_z) \times \exp\{\mathrm{i}[k\cos(\beta_z)\Delta z - \omega\Delta t]\}\sin(\beta_z)\, \mathrm{d}\beta_z\, \mathrm{d}\omega. \tag{4}$$

The angular aperture of the field depends on the distance z between the source plane and the observation region [$\theta = \theta(z)$]; however, this dependence is sufficiently smooth, and the field in the entire half-space $z > 0$ may be considered quasi-uniform. As pointed out in Ref. [5], in this case one can use Eqn (4) for the field correlation function, provided that the dependence of this function on z is taken into account.

Using Eqn (4) one can derive expressions for the function of temporal correlation (coherence) $\Psi_t(\Delta t, z)$ and the function of longitudinal spatial correlation $\Psi_{s\|}(\Delta z, z)$ of the field oscillations at the points P_1 and P_2:

$$\Psi_t(\Delta t, z) = \Psi_{\|}(\Delta t, \Delta z = 0, z) \sim \int_0^\infty \exp(\mathrm{i}\omega\Delta t) \int_0^\theta J(\omega, \beta_z)\sin(\beta_z)\, \mathrm{d}\beta_z\, \mathrm{d}\omega, \tag{5}$$

$$\Psi_{s\|}(\Delta z, z) = \Psi_{\|}(\Delta t = 0, \Delta z, z) \sim \int_0^\infty \int_0^\theta J(\omega, \beta_z) \exp[\mathrm{i}k\cos(\beta_z)\Delta z]\sin(\beta_z)\, \mathrm{d}\beta_z\, \mathrm{d}\omega. \tag{6}$$

From Eqn (5) one can obtain an expression for the frequency spectrum of the field in the region of observation (at the point z):

$$g(\omega,z) \sim \int_0^\infty \Psi_t(\tau,z)\exp(-i\omega\tau)\,d\tau = \int_0^\theta J(\omega,\beta_z)\sin(\beta_z)\,d\beta_z, \quad (7)$$

which formally describes the effect of diffraction-caused change of the field frequency spectrum (Wolf effect) in the process of its propagation in space [27, 28].

Expression (6) can be written in the formalised form [29, 30]:

$$\Psi_{s\|}(\Delta z,z) \sim \int_0^\infty w(k_z,z)\exp(ik_z\Delta z)\,dk_z, \quad (8)$$

where

$$k_z = \frac{\omega}{c}\cos\beta_z \quad (9)$$

is the cyclic spatial frequency of the wave field in the longitudinal direction (longitudinal spatial frequency), i.e., the projection of the wave vector of the spatial field component onto the z axis (Fig. 2); and $w(k_z,z)$ is the spectrum of longitudinal spatial frequencies of the field in the region of observation.

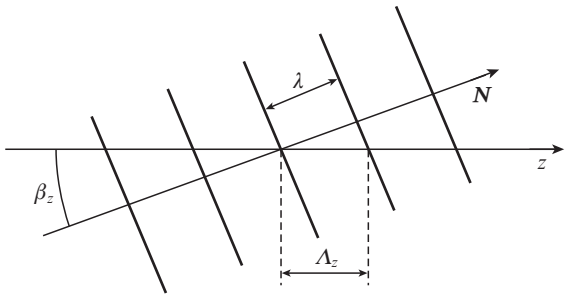

Figure 2. Spatial period $\Lambda_z = 2\pi/k_z = \lambda/\cos\beta_z$ of an angular component of the optical field along the longitudinal axis z.

From Eqn (8), assuming that the longitudinal spatial frequency spectrum is uniform, $w(k_z) = w_0 = \text{const}$, the expression for the longitudinal spatial coherence length was derived in the simple and memorable form [29, 30]

$$\frac{1}{L_c} \approx \frac{\Delta k_z}{2\pi} = \frac{1}{l_c} + \frac{1}{\rho_\|}, \quad (10)$$

where $\Delta k_z = k_{z\max} - k_{z\min}$ is the width of the spectrum $w(k_z,z)$ of the longitudinal spatial frequencies; $l_c \approx \lambda_0^2/\Delta\lambda$ is the temporal coherence length; λ_0 is the mean wavelength; $\Delta\lambda$ is the width of the frequency spectrum expressed in terms of the wavelength; and

$$\rho_\| = \frac{\lambda_0}{2\sin^2(\theta/2)} \quad (11)$$

is the longitudinal spatial correlation length, determined by the width of the field angular spectrum at $\Delta\lambda \to 0$. For small angles θ Eqn (11) turns into Eqn (2).

Expression (10) reflects the joint and competitive influence of the frequency and angular spectra on the longitudinal spatial correlation properties of the wave field. If $l_c \gg \rho_\|$, then, as follows from Eqn (10), the longitudinal spatial correlation length $L_c \approx \rho_\|$ is mainly determined by the angular spectrum of the field. On the contrary, if $l_c \ll \rho_\|$, then $L_c \approx l_c$ is mainly determined by the frequency spectrum of the field. If the values of l_c and $\rho_\|$ are comparable, then the longitudinal spatial correlation length L_c is equally determined by both the angular and frequency spectra of the field and is essentially different from both l_c and $\rho_\|$. Thus, for $l_c \approx \rho_\|$ the longitudinal spatial correlation length is two times smaller than each of these quantities: $L_c \approx 0.5 l_c \approx 0.5\rho_\|$

Expressions (6) and (8) define the general form of the spatial correlation function depending on the frequency-angular spectrum $J(\omega,\beta_z)$ or the spectrum of longitudinal spatial frequencies $w(k_z)$. However, the explicit form of these spectra depends on the particular source characteristics that specify the wave field in the observation area, namely, the source frequency spectrum, the field distribution over the source surface and the degree of the field correlation in the source plane.

3. Experimental study of the longitudinal correlation properties of the field generated by an extended broadband source

To study the longitudinal spatial correlation of a wave field one has to separate the initial field into two identical fields and superpose them after introducing a longitudinal spatial shift. This can be implemented using an interferometer with the amplitude division of the initial field, e.g., the Michelson interferometer with planar mirrors, one of which can be shifted along the optical axis of the interferometer [10, 29–31]. The methodology of performing the experiment on observation of the effects of longitudinal spatial correlation in a wave filed is based on the assertion that in the equal-arm Michelson interferometer the longitudinal shift Δz_M of one of the mirrors rives rise to a longitudinal spatial shift Δz between the interfering fields rather than a temporal delay $\Delta t = \Delta z/c$ [31]. Hence, in the Michelson interferometer the longitudinal shift of one of the mirrors reveals the longitudinal spatial correlation rather than the temporal coherence of the initial field.

Figure 3 presents the optical scheme intended for the study of the longitudinal spatial correlation in the free space, i.e., without any imaging optical elements. In this space the angular aperture of the field varies monotonically along its main direction of propagation (along the z axis):

$$\theta(D_S,z) = \arctan(0.5D_S/z), \quad (12)$$

where D_S is the diameter of the field source; and z is the distance from the field source (the image of the extended source S in the fixed mirror M1 of the interferometer) to the point photodetector PD placed at the optical axis of the interferometer.

In the free space the longitudinal spatial correlation length also varies monotonically. Figure 4a presents the interference pulse of longitudinal spatial correlation, i.e., the interference signal having the envelope that is determined by the modulus of the longitudinal spatial correlation function, the angular aperture of the field at the observation point being θ = 0.08 rad. Figure 4b shows the free-space evolution of the longitudinal spatial correlation length of the field, which was defined as the half-width of the interference pulse at the half-maximum level scaled to the longitudinal spatial shift $\Delta z = 2\Delta z_M$ of the interfering fields at D_S = 16 mm. The initial

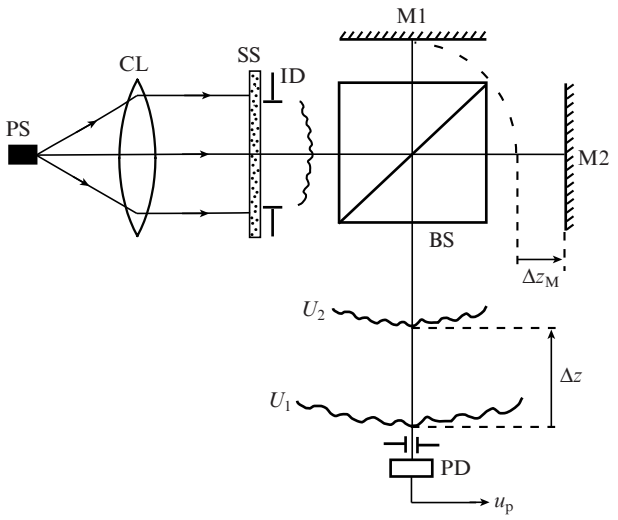

Figure 3. Michelson interferometer for observing the longitudinal spatial correlation effects in the free-space optical field:
(PS) primary light source; (CL) collimating lens; (SS) secondary extended light source (matted glass); (ID) iris diaphragm, limiting the dimensions of the extended source; (BS) beam splitter; (M1, M2) mirrors; (PD) point photodetector; u_p is the photoelectric signal; Δz_M is the longitudinal shift of the mirror M2; Δz is the relative longitudinal shift of interfering fields U_1 and U_2 at the interferometer output.

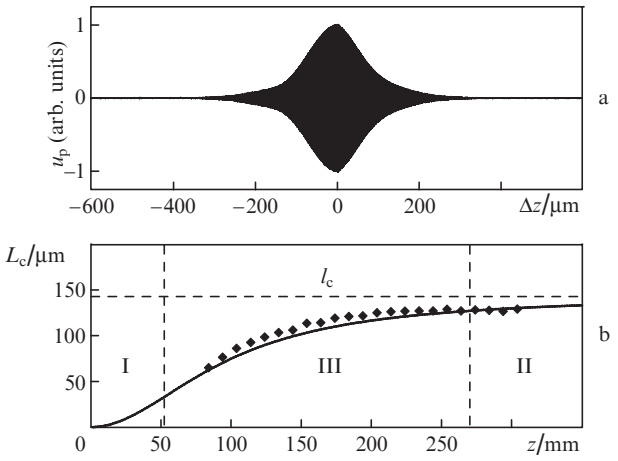

Figure 4. Interference pulse manifesting the longitudinal spatial correlation (a) and the evolution of the longitudinal spatial coherence length of the field in free space (without imaging optical elements) (b).

source was a superluminescent diode with $\lambda_0 = 0.827$ μm and $l_c \approx 143$ μm.

The experimental values of L_c (points) are in good agreement with the results of theoretical calculation using Eqn (10) (curves), and demonstrate the presence of three regions in the space where the optical field from the extended source propagates. The first region (I in Fig. 4b) is located near the field source; in this region the longitudinal spatial correlation is determined mainly by the angular spectrum of the field. The second region (II in Fig. 4b) is located in the far-field zone with respect to the source of the field. In this region the longitudinal spatial correlation is determined mainly by the frequency spectrum of the field. And, finally, between these regions there is the third region (III in Fig. 4b), in which the longitudinal spatial correlation is almost equally determined by both the angular and frequency spectra. Thus, we have theoretically and experimentally demonstrated the combined and competitive influence of the angular and frequency spectra on the longitudinal correlation properties of the optical field.

In addition to the study of longitudinal correlation properties of the field from an extended frequency-broadband light source in the free space, we also performed experimental and theoretical studies of the longitudinal spatial correlation properties of the field in the image space of a thin focusing lens [10, 32]. By the example of the field from a quasi-monochromatic source it was shown that, in contrast to the free-space case, in the image space the evolution of the longitudinal spatial properties of the field with a broad angular spectrum is non-monotonic. In this case the competition is observed between the effect of the extended light source dimensions and the effect of the dimensions of the imaging system aperture on the longitudinal spatial correlation properties of the field.

4. Effects of longitudinal spatial correlation of the wave field in interference microscopy

The interference microscopy [11–14] is used for non-destructive contactless investigation of the surface and inner structure of layered and weakly scattering objects of technological and medical origin with high spatial resolution. Therefore, for the development of this optical measurement method it is of primary importance to understand the mechanism of the interference microscope signal formation with the appropriate account for the effects, manifesting the longitudinal spatial correlation of the fields, one of which has passed through the object.

Being applied to the methods of interference microscopy that make use of the frequency-broadband light sources in combination with objectives having a large numerical aperture, expression (10) determines the longitudinal (along the optical axis) resolution of the interference microscope. In this case the maximal angular aperture of the object-probing field will be determined by the numerical aperture NA of the objective in the object arm:

$$\theta = \arcsin(\mathrm{NA}/n_0),$$

where n_0 is the refractive index of the immersion liquid.

The expression for the longitudinal resolution of the full-field interference microscope, formally similar to Eqn (10), was presented in Ref. [14], where it was obtained, most probably, by means of a semiempirical method. In [29, 30] expression (10) was derived in the analytical form by using the relation for the longitudinal spatial correlation function of the field having a uniform spectrum of longitudinal spatial frequencies.

Figure 5 shows the optical scheme of the interference microscope, using which we experimentally studied the effects of longitudinal spatial correlation of interfering fields with broad angular and frequency spectra, emerging in the interference microscopy.

Figure 6 presents the results of the experimental study of the interference microscope longitudinal resolution depending on the numerical aperture of the beam, probing the object, for two light sources with the frequency spectra of different width, namely, the semiconductor laser with $\lambda_0 = 0.808$ μm and $l_c \approx 300$ μm and the superluminescent diode with $\lambda_0 =$

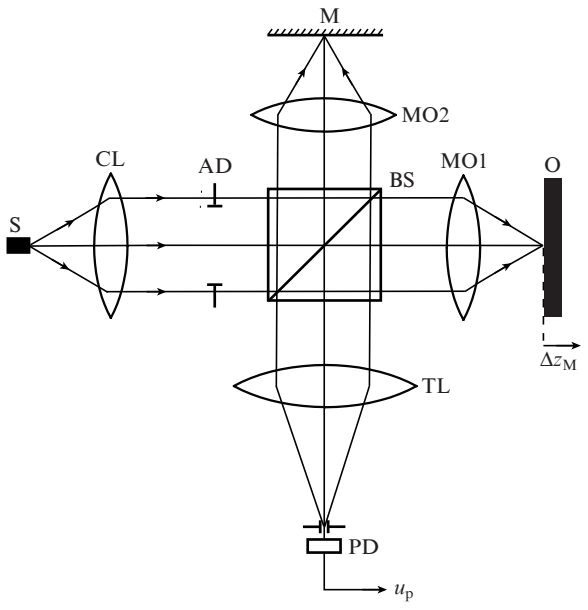

Figure 5. Optical scheme of the interference microscope with a focused beam of light used to illuminate the object:
(S) light source; (CL) collimating lens; (AD) aperture diaphragm; (BS) beam splitter; (M) reference mirror; (MO1, MO2) microscope objectives; (O) object; (TL) tube lens; (PD) photodetector; u_p is the photoelectric signal; Δz_M is the longitudinal shift of the object O with respect to the focus of the objective MO1.

0.833 μm and $l_c \approx 16.7$ μm. The numerical aperture of the probing beam was varied by changing the diameter of the aperture diaphragm AD. The theoretical curves in Fig. 6 are calculated using Eqn (10). The experimental results agree well enough with the theoretical dependences, obtained considering extended sources, which is an evidence of generality between the longitudinal correlation processes in the fields with a broad angular spectrum formed by the extended sources and by the optical elements with a large numerical aperture.

The fact that when $l_c \approx \rho_\parallel$ the longitudinal spatial correlation length L_c of the field becomes nearly two times smaller than each of the quantities l_c and $\rho_\parallel$ may be used to increase by two times the longitudinal resolution of the interference microscope, e.g., in surface micro-profilometry (the smaller the value of L_c, the greater the longitudinal resolution). Thus, at relatively small numerical apertures in the arms of an interference microscope one can achieve sufficiently large longitudinal resolution keeping the operating distance long enough, which is of importance, since the increase in the numerical aperture NA of a microscope objective reduces its operating distance.

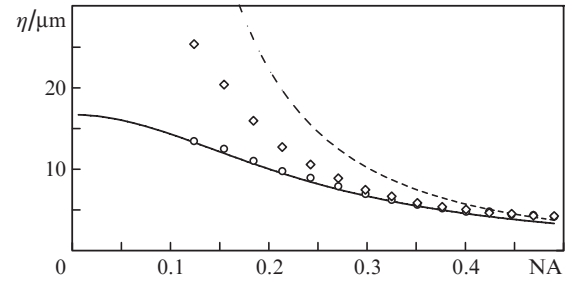

Figure 6. Dependences of the longitudinal resolution of the interference microscope η (full width of the interference signal at half-maximum along the axis Δz_M of the object) on the numerical aperture NA of the object-probing focused beam for two light sources with different widths of the frequency spectra, i.e., the semiconductor laser with $\lambda_0 = 0.808$ μm and $l_c \approx 300$ μm (◇, dashed curve) and superluminescent diode with $\lambda_0 = 0.833$ μm and $l_c \approx 16.7$ μm (○, solid curve). The points show experimental values, the curves plot theoretically calculated dependences.

Unfortunately, in the case of an interference microscope with a broadband light source and objectives with a large enough numerical aperture being used to perform depth-resolved probing of a layered object it is practically impossible to make use of the fact that at $l_c \approx \rho_\parallel$ the longitudinal spatial correlation length obeys the relation $L_c \approx 0.5 l_c \approx 0.5 \rho_\parallel$, because of the so-called defocusing effect [12, 20, 22–26, 33, 34]. In the interference microscopy this effect is explained by the non-coincidence of the focusing and the temporal coherence regions when a focused (converging) beam of broadband radiation passes through a boundary between the layers having different refractive indices within the object depth. This effect has been also studied by the example of the field from an extended source passing through a non-compensated planar layer of a medium in the unequal-arm Michelson interferometer [35, 36] and was referred to as 'the effect of recession of the pulses of temporal and spatial coherence'. However, both these names of the effect, as well as its physical interpretation, based on the competition of manifestations of temporal and spatial correlation of the fields in the longitudinal shift interferometry, are not correct within the framework of the conceptions, being developed in the present paper, i.e., the manifestation of the initial field longitudinal spatial correlation and the competitive influence of the angular and frequency spectra on this type of correlation in the longitudinal shift interferometer.

In our opinion, the nature of this effect is the following. Consider the field component (ray), propagating at the angle β_z with respect to the longitudinal axis z through the plane-parallel layer of the medium having the geometric thickness d and the refractive index n, immersed in a medium with the refractive index n_0 ($n_0 < n$) (Fig. 7). After passing the layer, the ray crosses the z axis at the point, shifted with respect to the position where it would cross the z axis in the absence of the layer by the distance

$$\delta z(\beta_z) = d\left(1 - \sqrt{\frac{n_0^2 - n_0^2 \sin^2\beta_z}{n^2 - n_0^2 \sin^2\beta_z}}\right). \qquad (13)$$

In the considered case ($n_0 < n$) the crossing point for the ray, passed through the layer, is shifted towards positive z val-

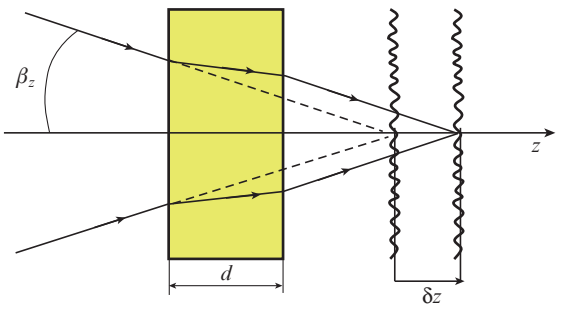

Figure 7. The angular component of the field, propagating at the angle β_z with respect to the z axis, passing through a plane-parallel layer.

ues, i.e., after passing the plane-parallel layer the field acquires a longitudinal forward shift with respect to the field in the absence of the layer. To estimate the resulting longitudinal shift of the field as a whole let us consider the displacement of its paraxial region

$$\delta\tilde{z} = \delta z(\beta_z \to 0) \approx d(n - n_0)/n. \quad (14)$$

At the same time, the wave field, passing through the layer, experiences a temporal delay due to the greater refractive index of the layer, which in the present case is optically denser than the surrounding medium ($n > n_0$). This temporal delay corresponds to an additional path difference, for estimation of which we also use the paraxial approximation:

$$\tilde{\Delta} \approx -d(n - n_0), \quad (15)$$

where the minus sign corresponds to the delay (time lag) of the field, passed through the medium, with respect to the field not passing the layer.

Therefore, it is possible to say that the angular spectrum ('sensitive' to the longitudinal shift) and the frequency spectrum ('sensitive' to the path difference) of the field oppositely affect the propagation of the field through the layer of substance, or, more precisely, through the boundaries of this layer [35, 36]. When passing through a layer of substance, the field with broad frequency and angular spectra experiences complex amplitude and phase transformations with respect to the field, not passed through such a layer. This leads to the mutual spatiotemporal decorrelation of these two fields, including that in the longitudinal direction. One can conventionally assume that the total decorrelation of the field in the longitudinal direction occurs under the condition

$$|\delta\tilde{z}| + |\tilde{\Delta}| > 0.5(l_c + \rho_{\parallel}). \quad (16)$$

In the interference experiment this decorrelation will manifest itself in the decrease in the amplitude of longitudinal spatial correlation pulse with increasing layer thickness d [35, 36], or its refractive index n (provided that the width of the frequency spectrum $\Delta\omega$ and the width of the angular spectrum θ are fixed), or increasing the width of any of these spectra (the parameters d and n of the layer are fixed).

For the variable component of the interference microscope signal (Fig. 5) with a broadband light source in the case of probing a single-layer object with the geometric thickness d and the refractive index n one can obtain the expression

$$u_p(\Delta z_M) \sim \mathrm{Re}[\Gamma_1(\Delta z_M) + \Gamma_2(\Delta z_M)], \quad (17)$$

where $\Gamma_1(\Delta z_M)$ and $\Gamma_2(\Delta z_M)$ are the functions of mutual correlation between the reference field and the fields, reflected from the front and back boundaries of the object layer, respectively, depending on the object shift Δz_M with respect to the focus of the object-probing beam:

$$\Gamma_1(\Delta z_M) \sim \int_{-\infty}^{+\infty} R_1 g(\lambda)\,\mathrm{sinc}\left(\frac{2\pi}{\lambda}\Delta z_M \frac{\mathrm{NA}^2}{2}\right) \times \exp\left[\mathrm{i}\frac{2\pi}{\lambda}2\Delta z_M\left(1 - \frac{\mathrm{NA}^2}{4}\right)\right]\mathrm{d}\lambda, \quad (18)$$

$$\Gamma_2(\Delta z_M) \sim \int_{-\infty}^{+\infty} R_2 T_1^2 g(\lambda)\,\mathrm{sinc}\left[\frac{2\pi}{\lambda}\left(\Delta z_M + \frac{dn_0}{n}\right)\frac{\mathrm{NA}^2}{2}\right] \times \exp\left\{\mathrm{i}\frac{2\pi}{\lambda}2\left[\Delta z_M + dn - \left(\Delta z_M + \frac{dn_0}{n}\right)\frac{\mathrm{NA}^2}{4}\right]\right\}\mathrm{d}\lambda, \quad (19)$$

where NA is the numerical aperture of the light beam, probing the object; R_1 and R_2 are the coefficients of reflection from the front and back layer boundaries; T_1 is the layer transmission coefficient; $\mathrm{sinc}\,x = \sin(x)/x$; and $g(\lambda)$ is the frequency spectrum of the broadband radiation source. Expressions (18) and (19) were derived using the diffraction transformations of the fields in the paraxial approximation.

Assume that the light source of the illuminating interferometer is almost strictly monochromatic, i.e., $g(\lambda) \approx g_0\delta(\lambda - \lambda_0)$, then

$$\Gamma_1(\Delta z_M) \sim R_1\,\mathrm{sinc}\left(\frac{2\pi}{\lambda_0}\Delta z_M \frac{\mathrm{NA}^2}{2}\right)\exp\left[\mathrm{i}\frac{2\pi}{\lambda_0}2\Delta z_M\left(1 - \frac{\mathrm{NA}^2}{4}\right)\right], \quad (20)$$

$$\Gamma_2(\Delta z_M) \sim R_2 T_1^2\,\mathrm{sinc}\left[\frac{2\pi}{\lambda_0}\left(\Delta z_M + \frac{dn_0}{n}\right)\frac{\mathrm{NA}^2}{2}\right] \times \exp\left\{\mathrm{i}\frac{2\pi}{\lambda_0}2\left[\Delta z_M + dn - \left(\Delta z_M + \frac{dn_0}{n}\right)\frac{\mathrm{NA}^2}{4}\right]\right\}. \quad (21)$$

In this case the signal of the interference microscope contains two interference pulses (peaks), corresponding to the front and back boundaries of the layer, at

$$\Delta z_M = 0, \quad \Delta z_M \approx \frac{dn_0}{n}, \quad (22)$$

The envelopes of these peaks are described by the function $\mathrm{sinc}\,x$, which, in turn, depends on the numerical aperture NA of the probing beam (the greater the NA, the narrower the interference peaks).

On the contrary, if we assume, that the numerical aperture of the beam, probing the object in the arm of the interference microscope, is small (NA $\to$ 0), then

$$\Gamma_1(\Delta z_M) \sim \int_{-\infty}^{+\infty} R_1 g(\lambda)\exp\left(\mathrm{i}\frac{2\pi}{\lambda}2\Delta z_M\right)\mathrm{d}\lambda, \quad (23)$$

$$\Gamma_2(\Delta z_M) \sim \int_{-\infty}^{+\infty} R_2 T_1^2 g(\lambda)\exp\left[\mathrm{i}\frac{2\pi}{\lambda}2(\Delta z_M + dn)\right]\mathrm{d}\lambda. \quad (24)$$

In this case the microscope signal contains two interference pulses, corresponding to the front and back boundaries of the layer, at

$$\Delta z_M = 0, \quad \Delta z_M \approx dn \quad (25)$$

with the envelopes determined by the particular form of the frequency spectrum $g(\lambda)$ of the light source and its width $\Delta\lambda$ [the greater the $\Delta\lambda$, the narrower the interference pulses (peaks)].

Thus, from the comparison of Eqns (22) and (25) it is seen that the angular spectrum of the field probing a layered object (determined by NA) and its frequency spectrum (characterised by $\Delta\lambda$) predetermine the appearance of the interference pulse from the back boundary of the layer object in the interference microscope signal at two different points on the longitudinal shift axis Δz_M of the object, separated by the distance

$$\Delta z_{M1} \approx dn - \frac{dn_0}{n} = \frac{d(n^2 - n_0)}{n}, \quad (26)$$

which causes the considered effect of decorrelation in the interference microscope, leading to essential amplitude reduction of the pulse from the back boundary of the layer, when

using a frequency-broadband light source in combination with wide-aperture objectives in this microscope. It is worth noting, that

$$\Delta z_{M1} \approx |\delta\tilde{z}| + |\tilde{\Delta}|. \quad (27)$$

Figure 8 presents the variable components of the signal of the interference microscope, the scheme of which is shown in Fig. 5, for a two-layer object at two values of the numerical aperture of the beam, probing such an object. The object was a thin-wall cuvette, consisting of a microscope cover glass glued to an optical aluminium-coated mirror by means of a double-sided sticky tape that played the role of a spacer for the air gap between the cover glass and the reflecting metallised surface of the mirror. The thickness of the cover glass was $d_1 = 170 \pm 1$ μm, the refractive index was $n_1 \approx 1.51$, the thickness of the air gap was $d_2 = 95 \pm 1$ μm, the refractive index of air was $n_2 \approx 1$. No immersion was used in this experiment, so that $n_0 \approx 1$. The light source was a superluminescent diode ($\lambda_0 = 0.831$ μm, $\Delta\lambda = 0.0164$ μm). The decrease in the signals, corresponding to the layer interfaces inside the object (glass–air and air–metal), under the increase in the numerical aperture of the probing beam is clearly seen.

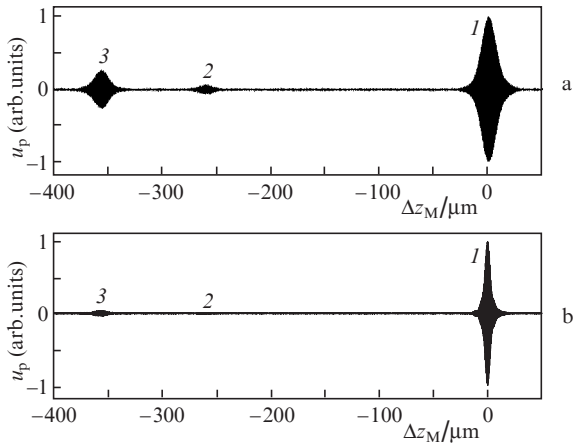

Figure 8. Signals of the interference microscope with illumination of the object with a focused light beam from a double-layered microscopic object, the numerical apertures of the object-probing beam being NA = (a) 0.12 and (b) 0.50. The figures denote the signals from the interfaces: air–glass (*1*), glass–air (*2*) and air–metal (*3*).

5. Method for compensating decorrelation effect, caused by the opposite influence of the angular and frequency spectra on the interferometer signal

In the interference microscopy the amplitude reduction of the signals coming from layer interfaces inside the object, that arises when combining a broadband source with objectives with a large numerical aperture, is to be somehow compensated, e.g., by changing the length of the interferometer object arm [14] by the value Δz_{M1}, determined by Eqn (26), or by using different numerical methods at the stage of the computer procession of the interference signal [33, 34, 37]. In Refs [24–26] it is proposed to fight this effect using a narrowband source; however, this method is unable to provide a complete elimination of the decorrelation effect, since the increase in the probing beam numerical aperture gives rise to spherical aberration that leads to the decrease in the amplitude and spreading of interference pulses, corresponding to the interfaces inside the object [38]. In Refs [39–42] the effect of opposite influence of the angular and frequency spectra on the interferometer signal formation is used for simultaneous determination of the geometric thickness and the refractive index.

The procedure of simultaneous determination of geometric thickness and refractive index of a single-layer object is reduced to the sequential focusing of the object beam, first, on the front boundary and, second, on the back one. Then the axial distance is measured between the positions Δz_M given by Eqn (22). At the second stage of the procedure the length of the reference arm is changed by the value Δz_{M1}, determined by expression (26); the criterion of matching the mentioned value of the reference arm length is the observation of the maximal amplitude of the interference microscope signal from the back surface of the layer. Thus we obtain two measured quantities that allow the calculation of the desired values of d and n of the layer using Eqns (22) and (26), provided that n_0 is known. Equations (22) and (26) were derived under the assumption that the refractive index n of the investigated layer is independent of the light frequency (wavelength), which is, generally, not true when using frequency-broadband radiation. Using different techniques, it is possible to take the dependence $n(\lambda)$ into account [41, 42], which allows determination of the geometric thickness and the refractive index with relative accuracy of ~0.1% [42]. For the refractive index this means uncertainty in the third digit after the decimal point.

To compensate the considered decorrelation effect we propose to use an illuminating interferometer with a broadband light source [43], in which the arm difference is given by expression (26), as a light source for the interference microscope. The schematic diagram of such interference system is presented in Fig. 9.

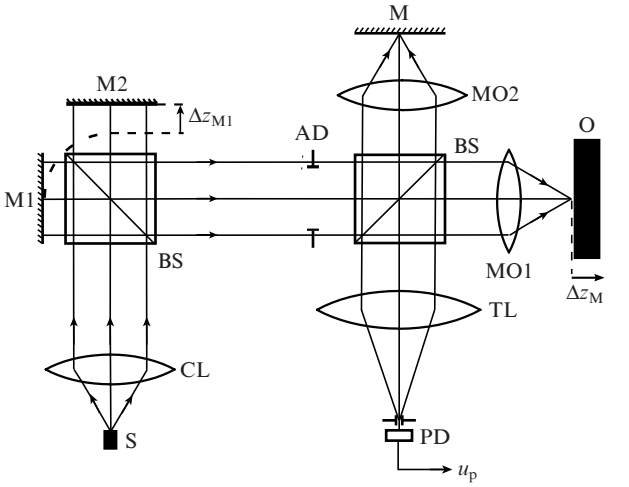

Figure 9. Optical scheme of the interference microscope with an illuminating interferometer:
(S) broadband light source; (CL) collimating lens; (AD) aperture diaphragm; (BS) beam splitters; (M1, M2, M) mirrors; (MO1, MO2) microscopic objectives; (O) object; (TL) tube lens; (PD) photodetector; u_p is the photoelectric signal; Δz_M is the longitudinal shift of the object O with respect to the focus of the objective MO1; Δz_{M1} is the compensating shift of the illuminating interferometer mirror.

Figure 10 shows the envelopes of interference signals from the measuring interferometer-microscope at different values Δz_{M1} in the arms of the illuminating interferometer. As an object we used the same thin-layered cuvette as in the previous experiment (see Fig. 8).

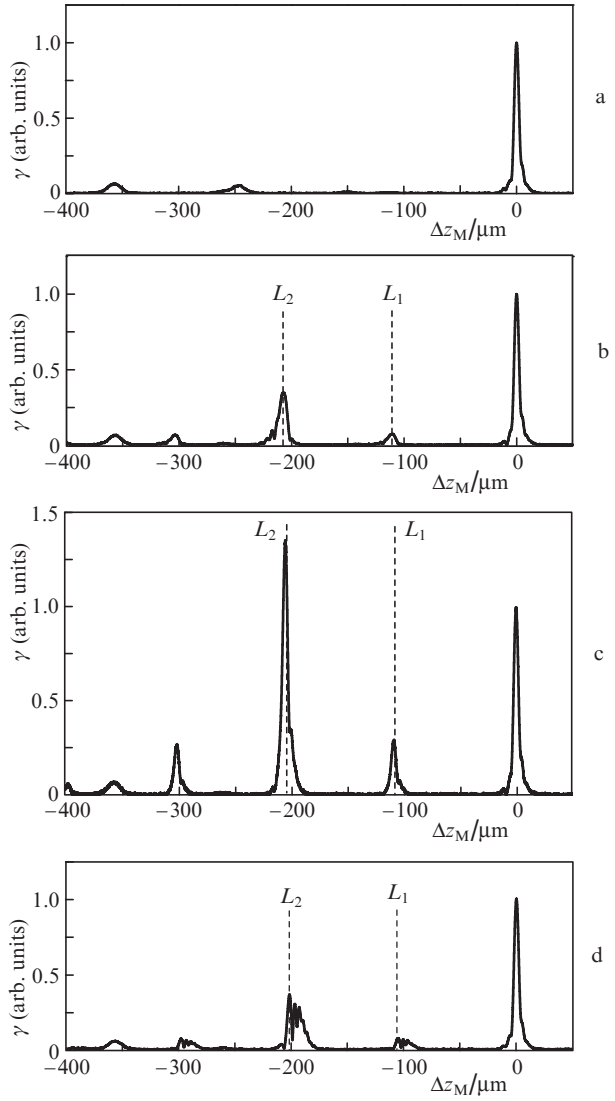

Figure 10. Envelopes (modulation coefficients γ) of the measuring interference microscope signal for the shift in the arms of the illuminating interferometer Δz_{M1} = (a) 138 ± 20, (b) 163 ± 20, (c) 175 ± 20 and (d) 188 ± 20 μm at $L_1 \approx d_1/n_1 = 108 \pm 1$ μm; $L_2 = d_1/n_1 + d_2/n_2 = 205 \pm 1$ μm.

Following our scheme proposed here, the technique for determining the geometric thickness and the refractive index of the layer, including the case of the refractive index dispersion, is analogous to that considered above, except the only difference that the compensating arm length difference Δz_{M1} is introduced not in the measuring interference microscope itself, but in its illuminating part. This allows making the interference microscope sufficiently compact by replacing the standard illuminating system with an illuminating interferometer and using the present method with commercially produced interference microscopes, in which the construction does not provide the possibility to vary the reference arm length, like, e.g., in the Mirau interferometer [22, 23].

6. Conclusions

The results, presented in this paper, as we believe, complete and develop the conceptions related to the correlation properties of optical wave fields, determined by the combination of their angular and frequency spectra, and also develop theoretical and experimental understanding of how these properties manifest themselves in the interferometry of partially coherent light, in particular, the interference microscopy, when the frequency-broadband light sources are used together with the optical elements having large numerical apertures.

The longitudinal correlation properties of an optical field are, generally, determined by both the frequency and the angular spectra of the field. The influence of these spectra on the longitudinal field correlation is joint and competitive in its nature. In application to interference microscopy this means simultaneous dependence of the longitudinal resolution on both the width of the frequency spectrum of the radiation used, and the numerical aperture of the objectives in the arms of the microscope. In the case of equal influence of the angular and frequency spectra on the field longitudinal correlation, when $\rho_{\|} \approx l_c$, the longitudinal correlation length appears to be by nearly two times smaller than each of these quantities, i.e., $L_c \approx 0.5\rho_{\|} \approx 0.5 l_c$. This effect can be used to increase approximately by two times the longitudinal resolution of the interference microscope in the profilometry of the object surface.

When the field with broad angular and frequency spectra passes through a plane-parallel layer of the medium, the decorrelation of this field occurs with respect to the field that did not pass through such a layer. This decorrelation is caused by the opposite influence of the angular and frequency spectra on the spatiotemporal correlation properties of the field. In the interference microscopy of layered objects this effect leads to a decrease in the amplitudes of the signals from the layer interfaces inside the object, till they completely vanish against the background of the noises of the detecting electronic instrumentation, as the numerical aperture of the object-probing light beam is being increased.

We propose a method for compensating the considered decorrelation effect using the illuminating interferometer with a frequency-broadband light source, playing the role of a light source for the interference microscope. By varying the arm length difference in the illuminating interferometer it becomes possible to compensate the decorrelation effect in the measuring interference microscope, to increase the amplitude of the signals from layer interfaces inside the object, and, thus, to detect and determine these interfaces. Measuring the distance between the interference peaks, corresponding to the boundaries between the layers inside the object together with the compensating arm length difference in the illuminating interferometer allows the solution of the problem of simultaneous determination of the thickness and refractive index of layers inside the object using no *a priori* information about their parameters. The proposed optical scheme with the illuminating interferometer possesses a number of advantages as compared to the analogous systems, since the compensating changes of the arm length are performed in the illuminating interferometer, keeping unperturbed the measuring interference microscope itself.

Acknowledgements. The work was carried out under partial support from the Federal Target Program 'Scientists and Science Educators of Innovative Russia' (Grant No. 14.

B37.21.0728) and the President Grant for Government Support of Leading Scientific Schools of the Russian Federation (Grant No. NSh-1177.201202).

References

1. Born M., Wolf E. *Principles of Optics* (Cambridge: Cambridge University Press, 1997).
2. Mandel L., Wolf E. *Optical Coherence and Quantum Optics* (Cambridge: Cambridge University Press, 1995).
3. Françon M., Mallick S. *Appl. Opt*., **6**, 873 (1967).
4. Soroko L.M. *Holography and Coherent Optics* (New York: Plenum Press, 1980).
5. Rytov S.M., Kravtsov Yu.A., Tatarskii V.I. *Principles of Statistical Radiophysics. Vol. 2. Correlation Theory of Random Processes* (Berlin: Springer-Verlag, 1987).
6. Zarubin A.M. *Opt. Commun*., **100**, 491 (1993).
7. Rosen J., Yariv A. *Opt. Commun*., **117**, 8 (1995).
8. Wolf E. *Opt. Lett*., **19**, 2024 (1994).
9. Lokshin G.R., Uchenov A.V., Entin M.A. *Radiotekh. Elektron*., **97**, 416 (2000) [*J. Commun. Tech. Electron*., **45**, 384 (2000)].
10. Ryabukho V., Lyakin D., Lobachev M. *Opt. Lett*., **29**, 667 (2004).
11. Sheppard C.J.R., Roy M., Sharma M.D. *Appl. Opt.*, **43**, 1493 (2004).
12. Aguirre A.D., Fujimoto J.G., in *Optical Coherence Tomography. Technology and Applications* (Berlin: Springer, 2008) p. 505.
13. Dubois A., Vabre L., Boccara A.C., Beaurepaire E. *Appl. Opt*., **41**, 805 (2002).
14. Dubois A., Boccara A.C., in *Optical Coherence Tomography. Technology and Applications* (Berlin: Springer, 2008) p. 565.
15. Rosen J., Takeda M. *Appl. Opt*., **37**, 4107 (2000).
16. Pavliček P., Halouzka M., Duan Z., Takeda M. *Appl. Opt*., **48**, H40 (2009).
17. Liu Z., Gemma T., Rosen J., Takeda M. *Appl. Opt*., **49**, D12 (2010).
18. Liu H., Han S. *Opt. Lett*., **33**, 824 (2008).
19. Ferri F., Magatti D., Sala V.G., Gatti A. *Appl. Phys. Lett*., **92**, 261109 (2008).
20. Abdulhalim I. *J. Opt. A: Pure Appl. Opt*., **8**, 952 (2006).
21. Zeylikovich I. *Appl. Opt*., **47**, 2171 (2008).
22. De Groot P., de Lega X.C. *Appl. Opt*., **43**, 4821 (2004).
23. De Groot P., de Lega X.C. *Opt. Lett*., **32**, 1638 (2007).
24. Safrani A., Abdulhalim I. *Appl. Opt*., **50**, 3021 (2011).
25. Safrani A., Abdulhalim I. *Opt. Lett*., **37**, 458 (2012).
26. Abdulhalim I. *Ann. Phys*., **524**, 787 (2012).
27. Gamliel A., Agrawal G.P. *J. Opt. Soc. Am. A*, **7**, 2184 (1990).
28. D'yakov Yu.E. *Kvantovaya Elektron*., **20**, 1068 (1993) [*Quantum Electron*., **23**, 931 (1993)].
29. Ryabukho V.P., Lyakin D.V, Lychagov V.V. *Opt. Spektrosk*., **107**, 300 (2009) [*Opt. Spectrosc.*, **107**, 282 (2009)].
30. Ryabukho V.P., Lyakin D.V., Grebenyuk A.A., Klykov S.S. *J. Opt*., **15**, 025405 (2013).
31. Ryabukho V.P., Lyakin D.V., Lychagov V.V. *Opt. Spektrosk*., **102**, 996 (2007) [*Opt. Spectrosc.*, **102**, 918 (2007)].
32. Lyakin D.V., Ryabukho V.P. *Pis'ma Zh. Tekh. Fiz*., **37**, 94 (2011) [*Tech. Phys. Lett*., **37**, 45 (2011)].
33. Labiau S., David G., Gigan S., Boccara A.C. *Opt. Lett*., **34**, 1576 (2009).
34. Binding J., Ben Arous J., Leger J.-F., Gigan S., Boccara C., Bourdieu L. *Opt. Express*, **19**, 4833 (2011).
35. Ryabukho V., Lyakin D., Lobachev M. *Opt. Lett*., **30**, 224 (2005).
36. Ryabukho V.P., Lyakin D.V., Lychagov V.V. *Opt. Spektrosk*., **100**, 807 (2006) [*Opt. Spectrosc.*, **100**, 724 (2006)].
37. Grebenyuk A.A., Ryabukho V.P. *Opt. Lett*., **37**, 2529 (2012).
38. Ryabukho V.P., Lychagov V.V., Lyakin D.V., Smirnov I.V. *Opt. Spektrosk*., **110**, 854 (2011) [*Opt. Spectrosc.*, **110**, 802 (2011)].
39. Tearney G.J., Brezinski M.E., Southern J.F., Bouma B.E., Hee M.R., Fujimoto J.G. *Opt. Lett*., **20**, 2258 (1995).
40. Fukano T., Yamaguchi I. *Opt. Lett*., **21**, 1942 (1996).
41. Maruyama H., Inoue S., Mitsuyama T., Ohmi M., Haruna M. *Appl. Opt*., **41**, 1315 (2002).
42. Kim S., Na J., Jin Kim M., Ha Lee B. *Opt. Express*, **16**, 5516 (2008).
43. Lyakin D.V., Lobachev M.I., Ryabukho V.P., Tuchin V.V. *Proc. SPIE Int. Soc. Opt. Eng*., **4956**, 163 (2003).